High-Precision Laser Dilatometry Precipitation Processes in Titanium and Aluminium Alloys

Method and Application

Martin Luckabauer
University of Twente, ET, MS3

Dilatometry – seemingly a well-known method

Determination of
thermal expansion:

$$L \cdot \alpha = \frac{\Delta L}{\Delta T}$$

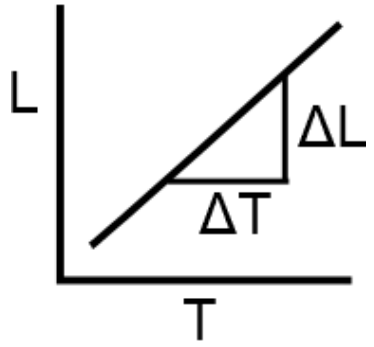

Additional volume effects:
e.g. First-order Phase transitions

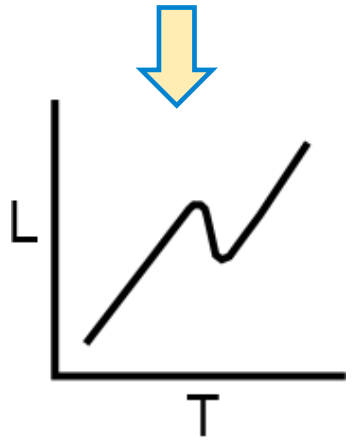

Advanced Techniques
Free-volume kinetics (vacancies etc.)

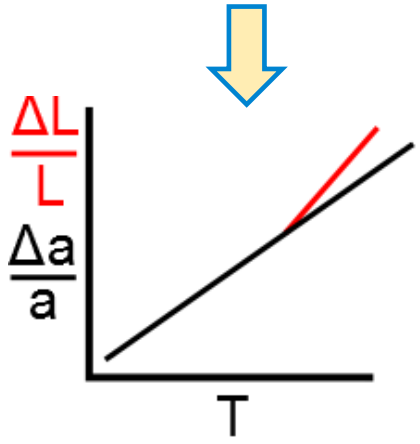

Special Techniques
Deformation Dilatometer
Quenching, etc.

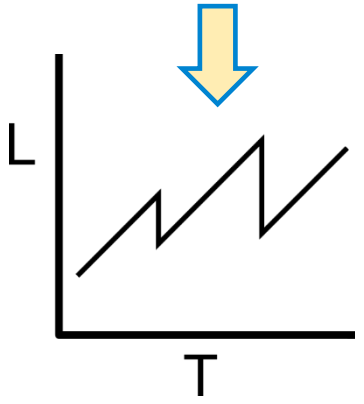

UNIVERSITY OF TWENTE.

Dilatometry – seemingly a well-known method

In theory dilatometry **is the ideal method** to **study thermodynamic processes** in materials:

Thermodynamic state variable
Volume [V]
easy to assess, **can be measured in absolute terms**

Thermodynamic state variable
Heat [Q]
practically inaccessible, **only changes are measurable**

Historically industry has put **very little effort in the improvement of Dilatometers, Calorimetry** (e.g. DSC) was **developed to a very advanced stage.**

Pressing needs and questions in modern materials science:

- **Precipitation kinetics** (multistage) **in complex alloys**
- **Defect annihilation and formation** (vacancies, dislocations, pores etc.)
- **Isothermal measurements with useful measurement stability**
- **Slow processes – long-time measurements**
- **Separation of kinetics and crystal lattice expansion** (modulation)
- **Optimized heating and cooling concepts**

…. Cannot be tackled by commercial equipment

The advanced dilatometry project

Project Goals:

- Fast and precise temperature control **exceeding the capabilities of available furnace concepts**
- **nm-resolution** without the need for special sample geometry, based on laser interferometry
- **Highest stability against environmental influences** by using the latest interferometer technology: SIOS SP120DI
- Full **implementation of sinusoidal temperature modulation** into the controller
- Possibility for sample cooling (quenching)

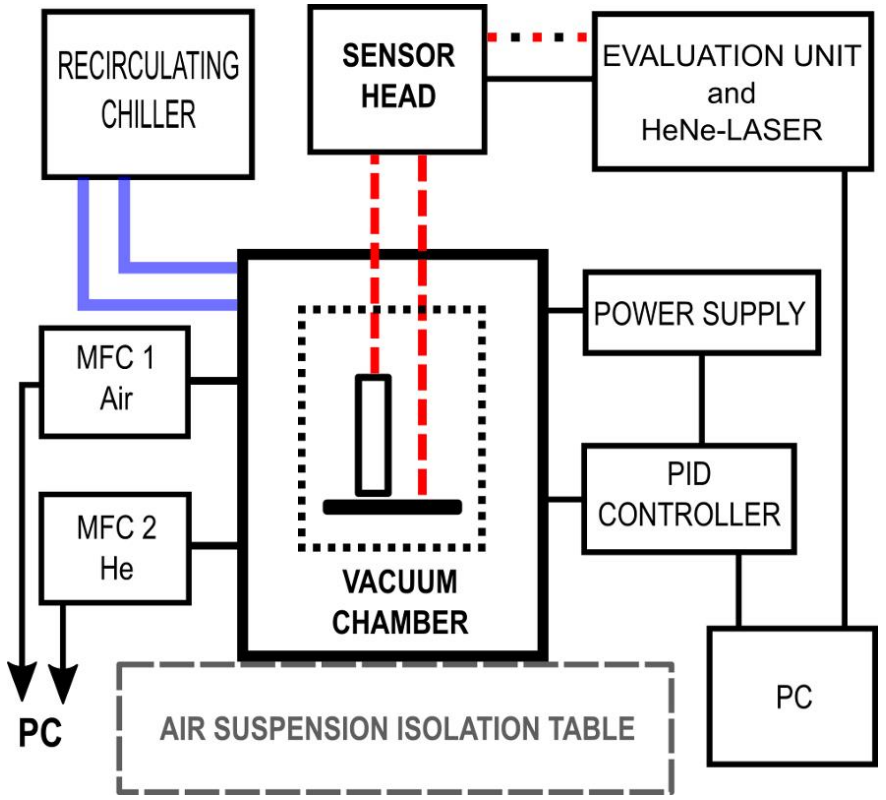

Furnace Concept

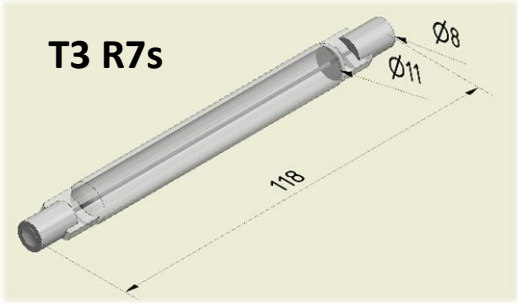

One possibility: **In-vacuum halogen lamp furnace**

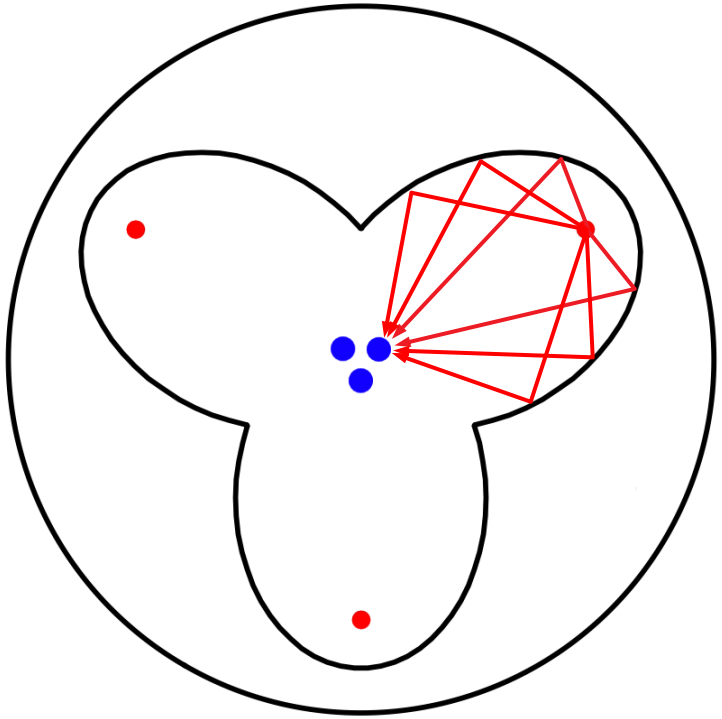

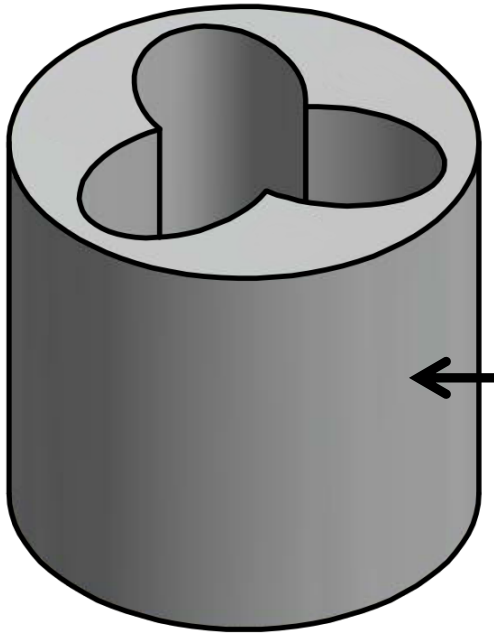

Aluminum Reflector with 3 nearly confocal elliptical cutouts

By using conventional 300 W Tungsten halogen lamps
very high energy densities can be reached

Furnace Concept

Advantages

- "Cold wall'' concept --> only Tungsten filament and sample (sample-holder) is heated. Water-cooled reflector stays at constant temperature.
- Control time constant is very low. Filament temperature change rate **> 1000 K/s --> no deadtime in the control loop.**
- Due to the radiation focusing a very high heat flux can be achieved
- No restrictions on the sample material

Large heat flux
+
low thermal inertia
=
Fast and precise control

Disadvantages

- Tight tolerances and mirror like surface finish > challenging to produce
- Halogen lamps cannot operate in vacuum > complex cooling design

The finished furnace / sample holder assembly

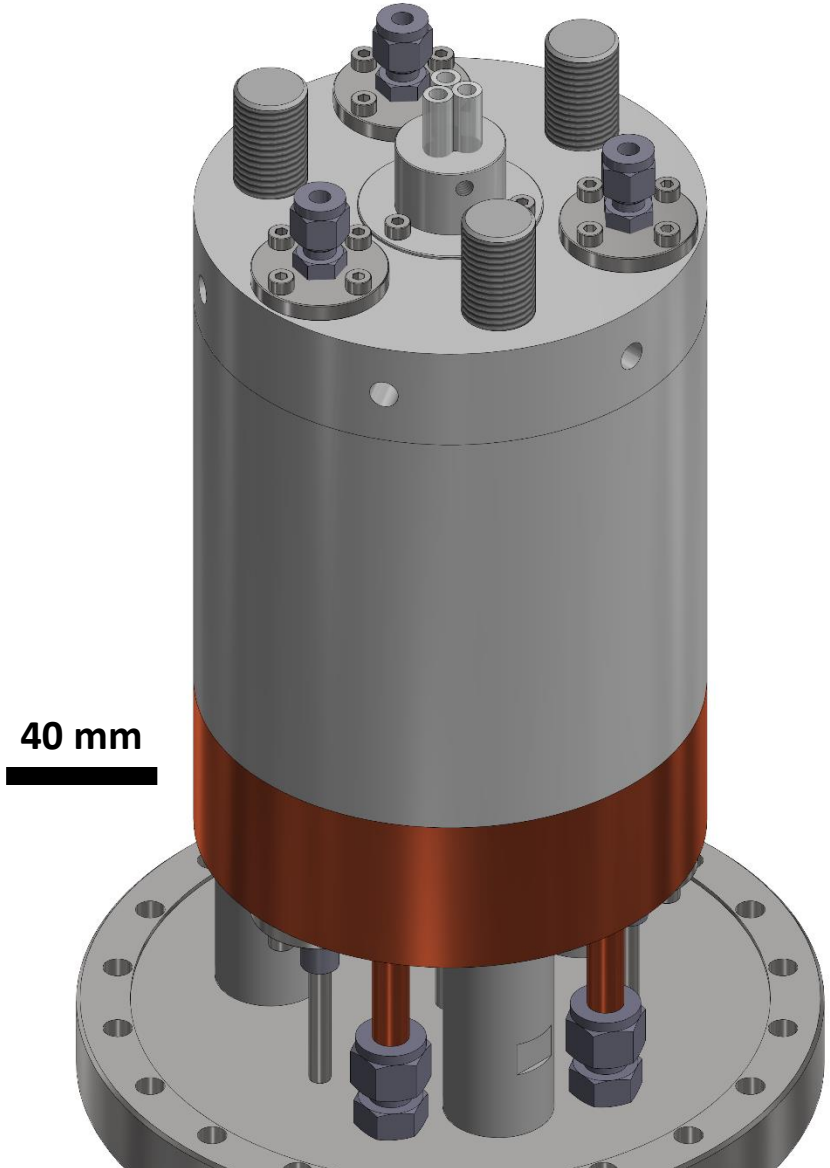

The finished furnace / sample holder assembly

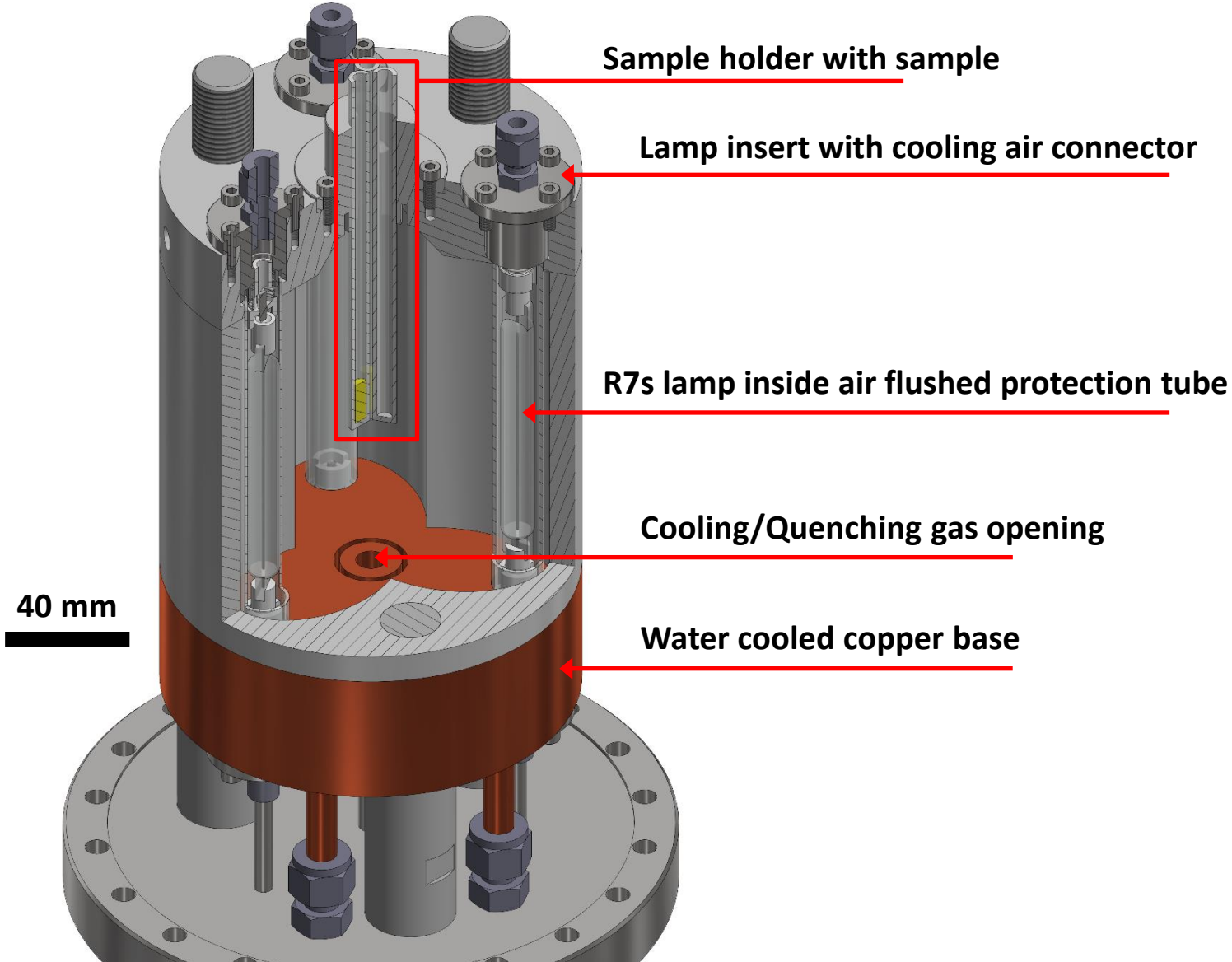

The finished setup

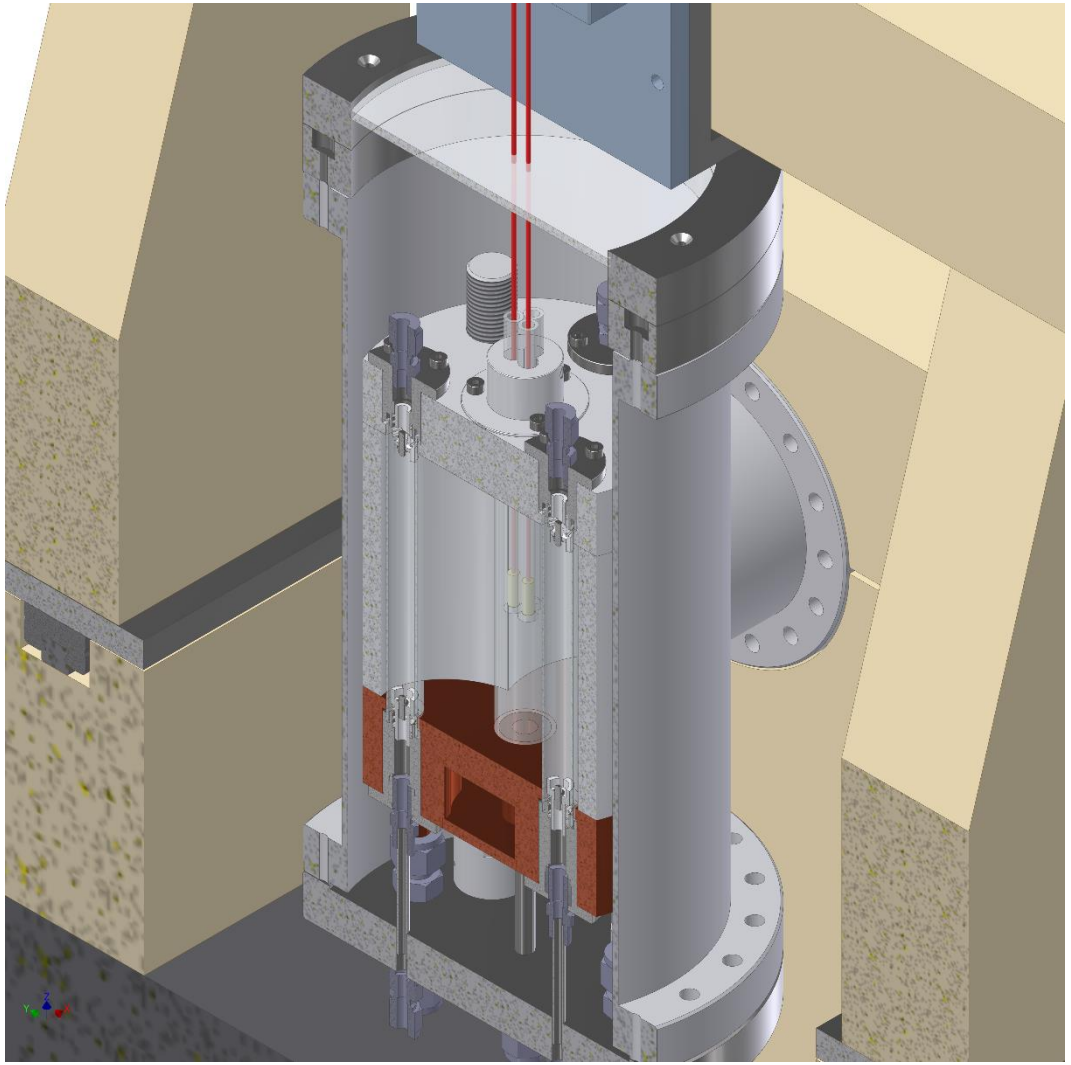

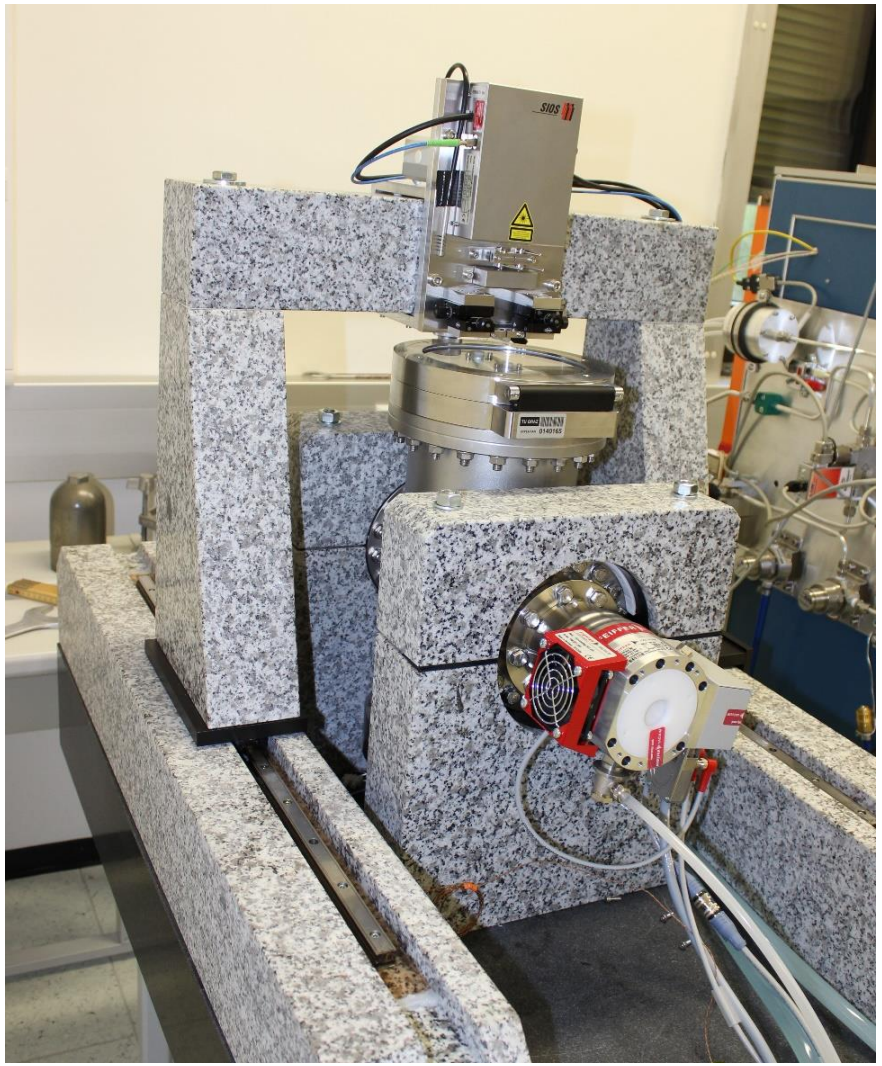

Case study 1:
Time-**T**emperature-**P**recipitation behavior
AW 6060

Precipitate formation in Al-Mg-Si (AW6060)

- **Al-Mg-Si** is one of the most widely used hardenable aluminum alloy systems.
- After solid solution annealing and quenching and depended on the annealing temperature, a variety of metastable phases form on the way to the stable Mg2Si phase.

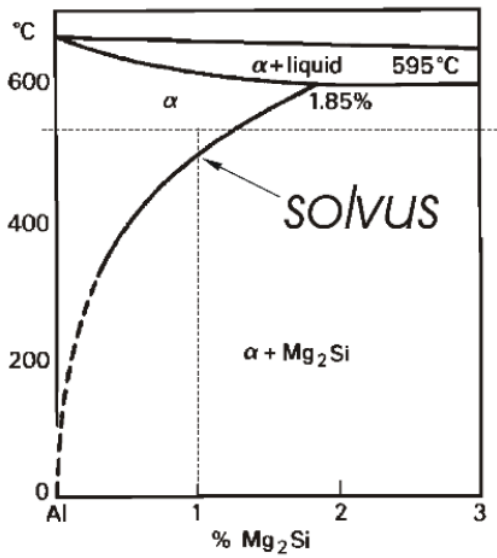

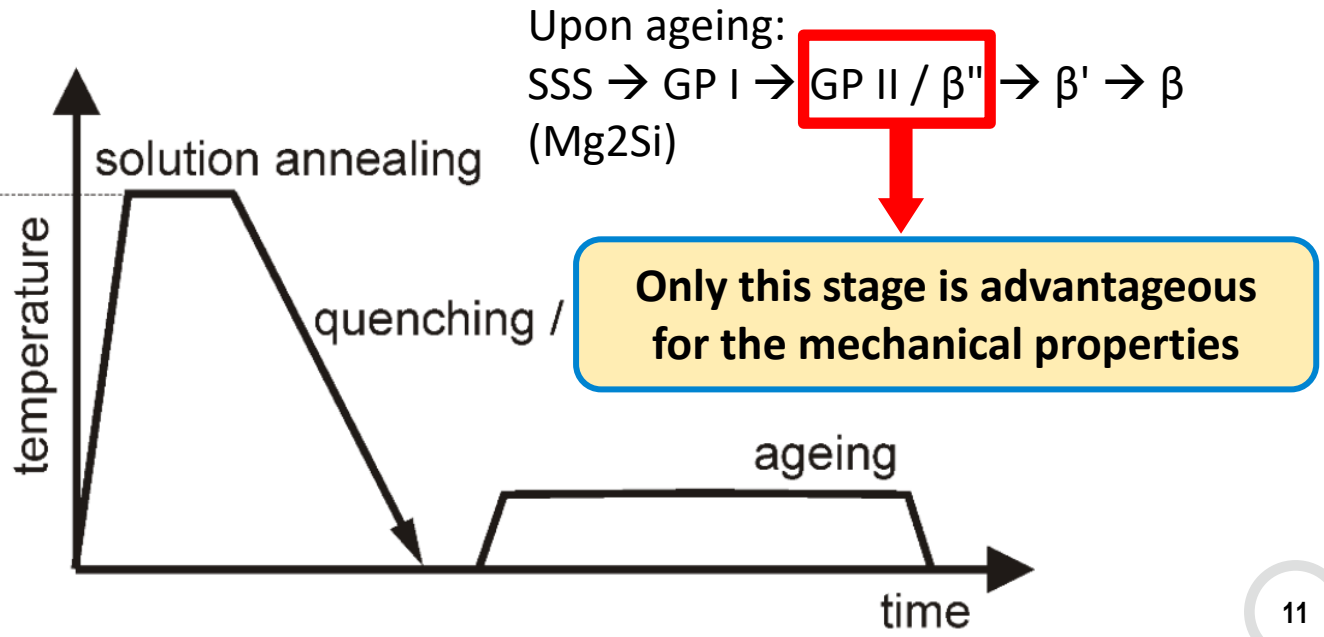

Upon ageing:
SSS → GP I → GP II / β" → β' → β
(Mg2Si)

Only this stage is advantageous for the mechanical properties

Precipitate formation in Al-Mg-Si (AW6060)

- In principle the **precipitation process causes an isothermal volume change** at the aging temperature.

- The direct observation of this volume change would directly depict the precipitation sequence and lead to the ideal time – temperature combination for a **maximum of β"-phase**.

- **HOWEVER:** The effect is expected to be in the **sub-µm regime** for reasonable sample sizes (< 30 mm) and takes **hours to days.**

Precipitate formation in Al-Mg-Si (AW6060)

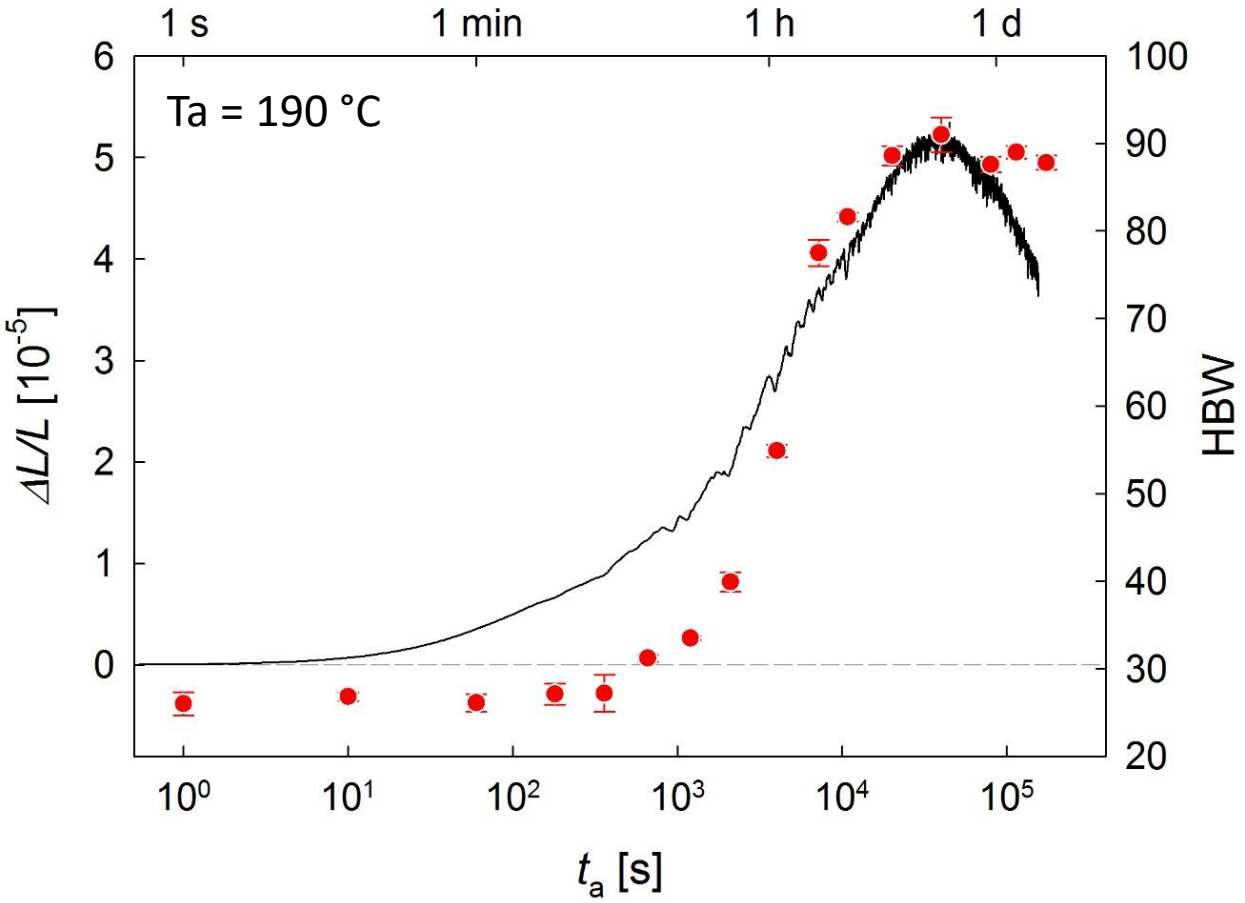

Complete heat treatment cycle was performed in the dilatometer:

Step 1	Solutionizing: 540 °C 25 min
Step 2	He-quench to RT
Step 3	Holding for 4 min
Step 4	Heating to variable annealing temperature at 300 K/min

The volume change is clearly visible and corresponds to the hardness change.

M. Luckabauer, E. Hengge, G. Klinser, W. Sprengel, R. Würschum, Magnesium Technology 2017 **1**, 669-674 2017

Precipitate formation in Al-Mg-Si (AW6060)

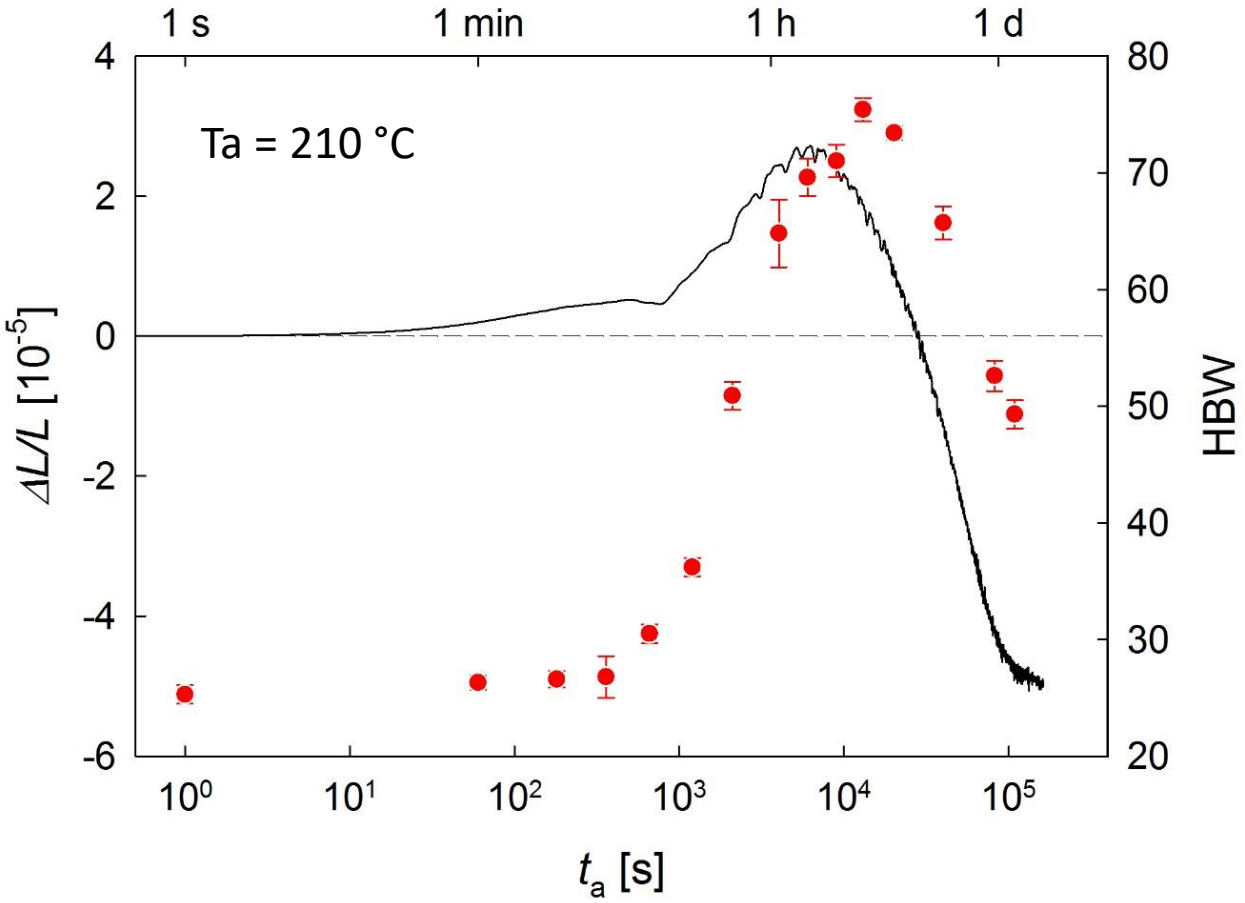

Complete heat treatment cycle was performed in the dilatometer:

Step 1	Solutionizing: 540 °C 25 min
Step 2	He-quench to RT
Step 3	Holding for 4 min
Step 4	Heating to variable annealing temperature at 300 K/min

The volume change is clearly visible and corresponds to the hardness change.

UNIVERSITY OF TWENTE.

M. Luckabauer, E. Hengge, G. Klinser, W. Sprengel, R. Würschum, Magnesium Technology 2017 **1**, 669-674 2017

Precipitate formation in Al-Mg-Si (AW6060)

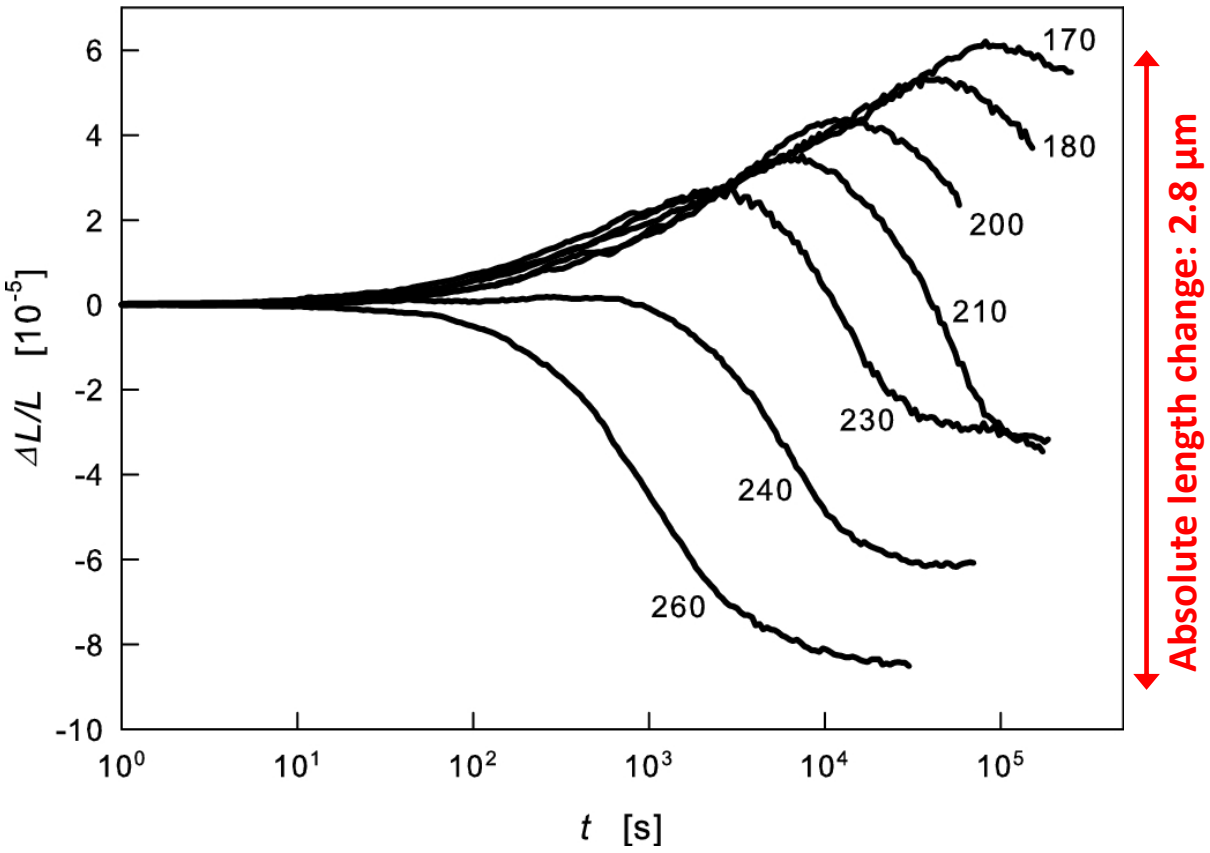

Complete heat treatment cycle was performed in the dilatometer:

Step 1	Solutionizing: 540 °C 25 min
Step 2	He-quench to RT
Step 3	Holding for 4 min
Step 4	Heating to variable annealing temperature at 300 K/min

The volume change is clearly visible and corresponds to the hardness change.

UNIVERSITY OF TWENTE.

M. Luckabauer, E. Hengge, G. Klinser, W. Sprengel, R. Würschum, Magnesium Technology 2017 **1**, 669-674 2017

Precipitate formation in Al-Mg-Si (AW6060)

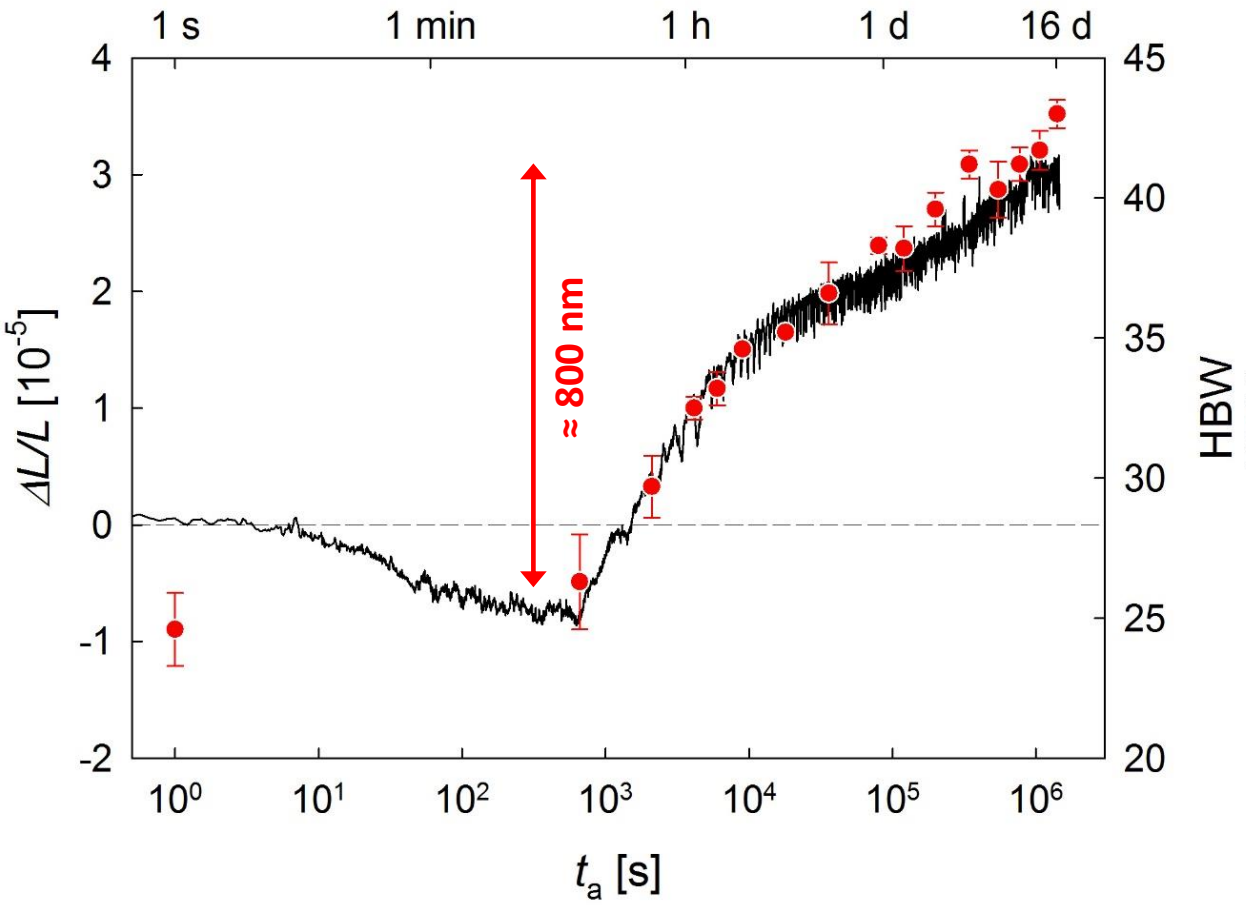

Complete heat treatment cycle was performed in the dilatometer:

Step 1	Solutionizing: 540 °C 25 min
Step 2	He-quench to RT
Step 3	Holding for 4 min
Step 4	Heating to variable annealing temperature at 300 K/min

The volume change is clearly visible and corresponds to the hardness change.

Phase formation process can be monitored down to rates of **0.5 nm/h**

UNIVERSITY OF TWENTE.

M. Luckabauer, E. Hengge, G. Klinser, W. Sprengel, R. Würschum, Magnesium Technology 2017 **1**, 669-674 2017

Precipitate formation in Al-Mg-Si (AW6060)

Analaysing the Results

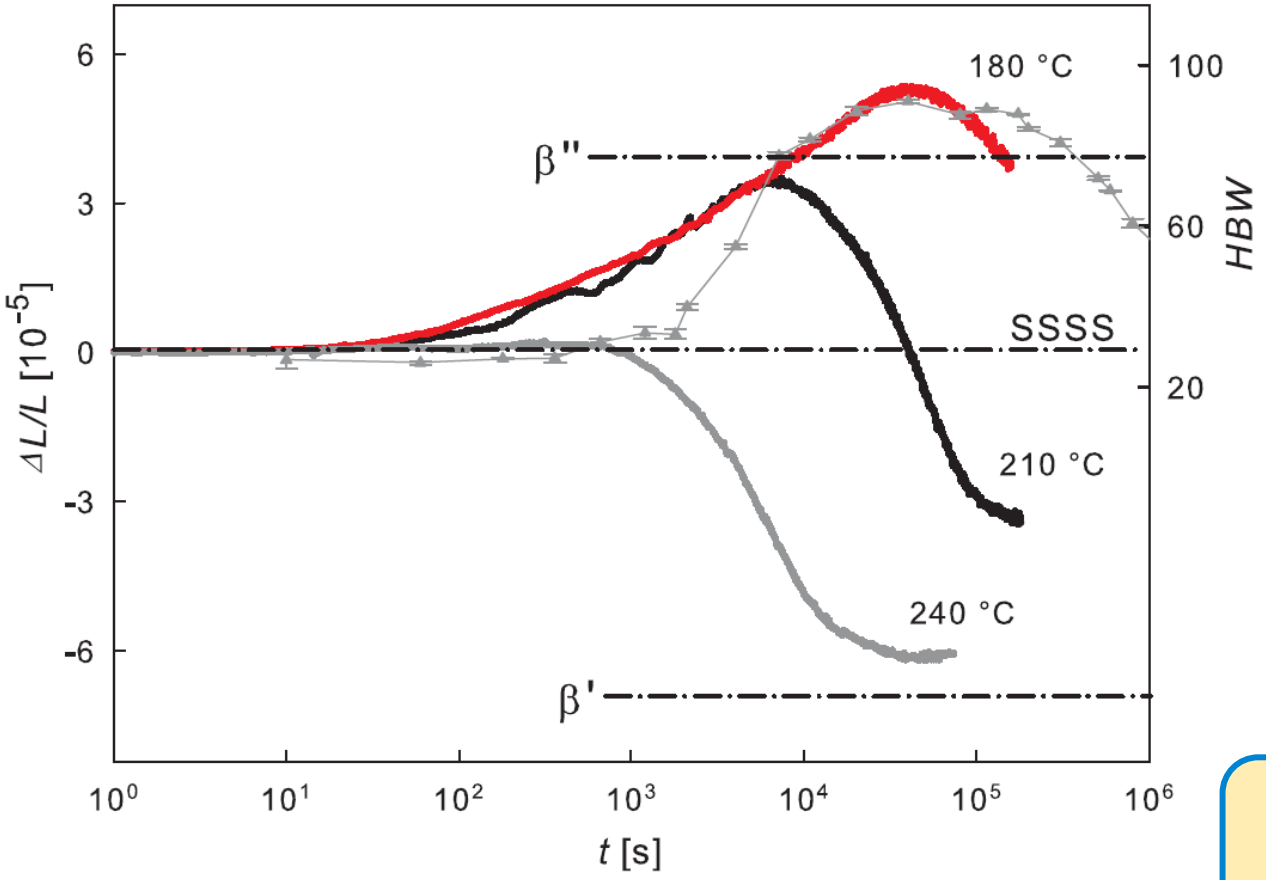

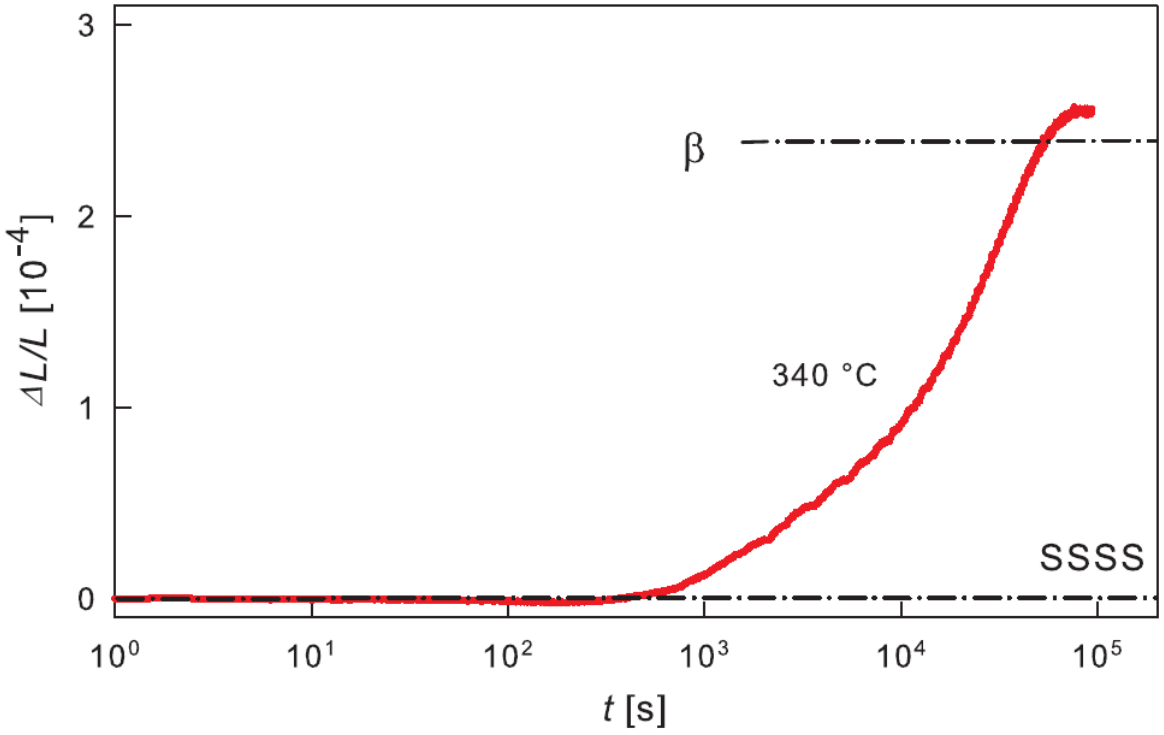

Theoretical volume changes based on the available alloy elements concentration can be compared to the measurement

E. Hengge, R. Enzinger, M. Luckabauer, W. Sprengel & R. Würschum, Philosophical Magazine Letters, **98:7**, 301-309, 2018

UNIVERSITY OF TWENTE.

TTP diagram Al-Mg-Si (AW6060)

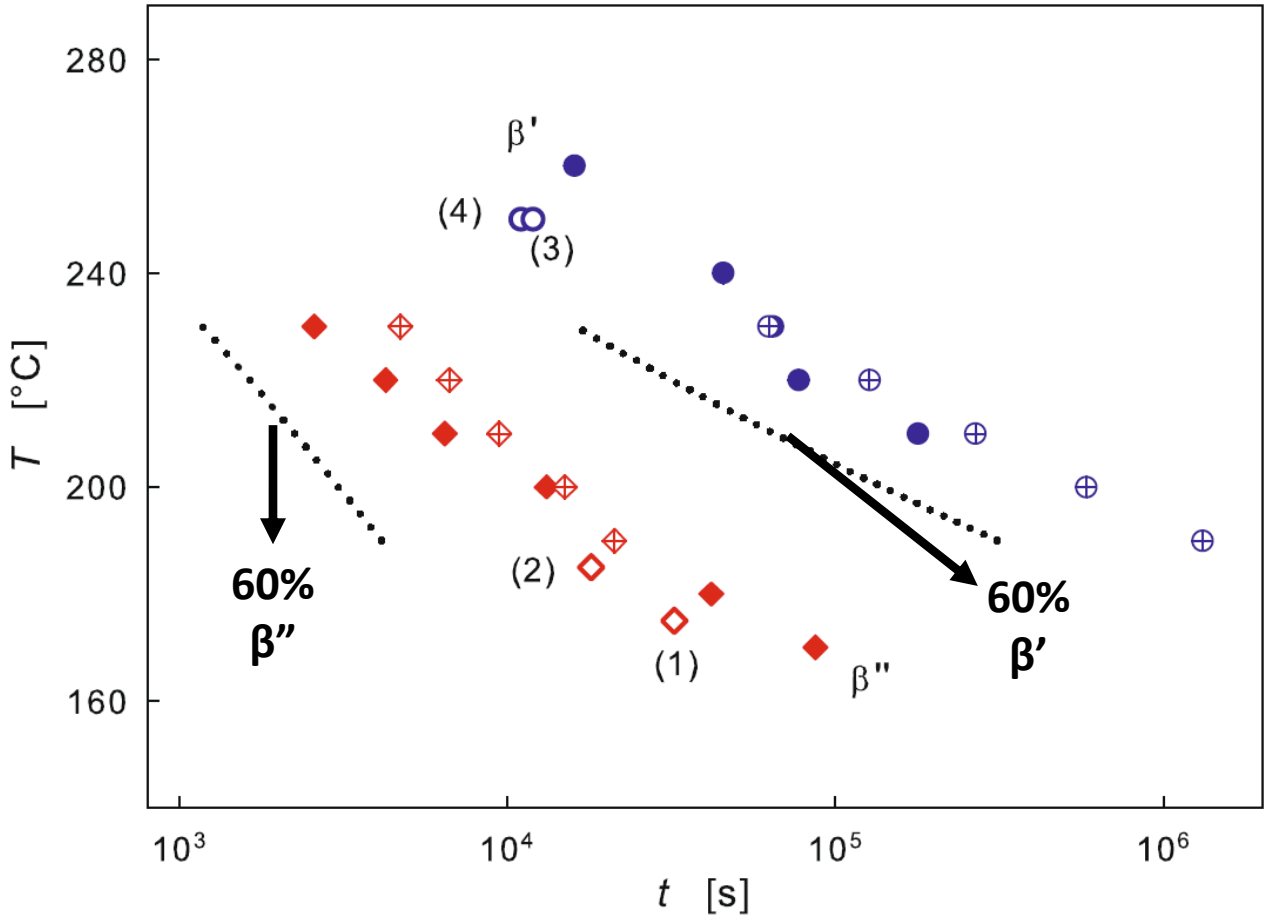

By analyzing the measurement results an

Isothermal TTP diagram can easily be drawn

Here the **symbols** correspond to **98% phase fraction** and the **dashed lines represent 60%**

R. Enzinger, E. Hengge, W. Sprengel *et al.* , J Mater Sci **54**, 5083–5091 2019

UNIVERSITY OF TWENTE.

Case study 2:
Influence of Oxygen on the Kinetics of ω and α Phase formation in β Ti-V

ω phase formation in β Ti matrix (Ti-21V)

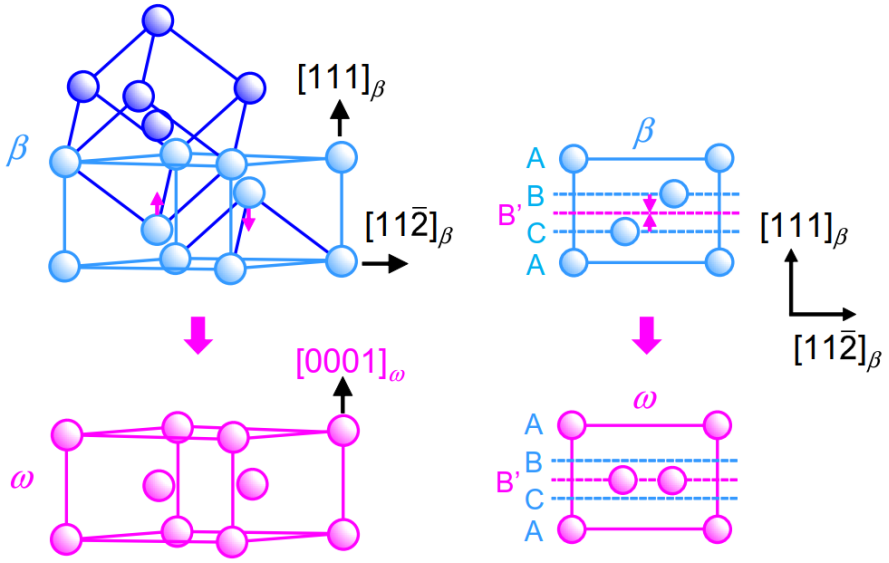

ω phase forms by a collapse of ever second (111) pair of the β phase

The formation of ω precipitates leads to **embrittlement**, often to a **total loss of ductility**

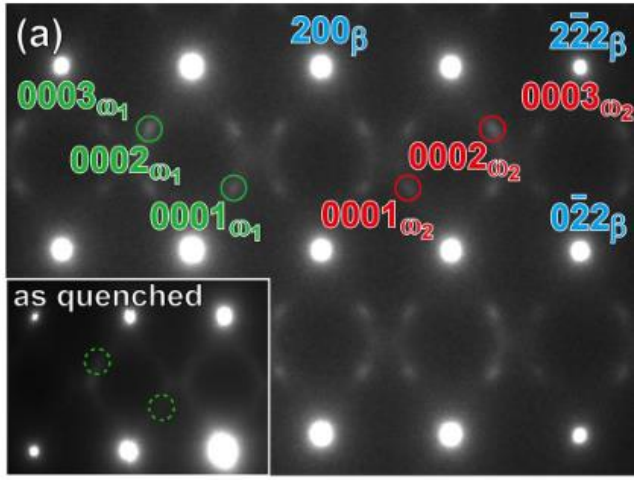

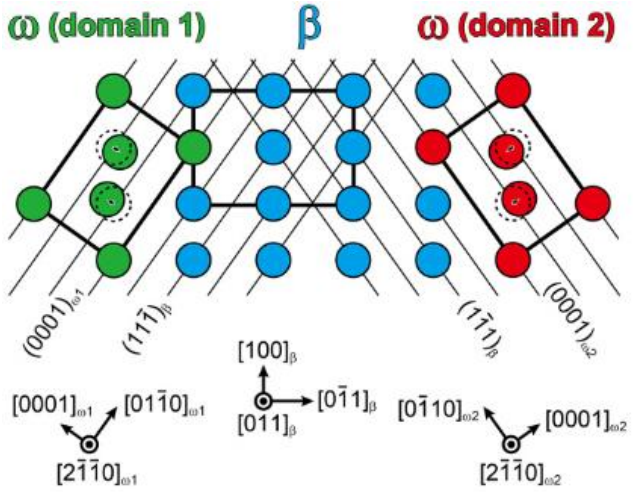

HAADF-STEM image taken along the [011] β direction
β phase (B: blue) and domains 1 (G: green) and 2 (R: red) of the ω phase

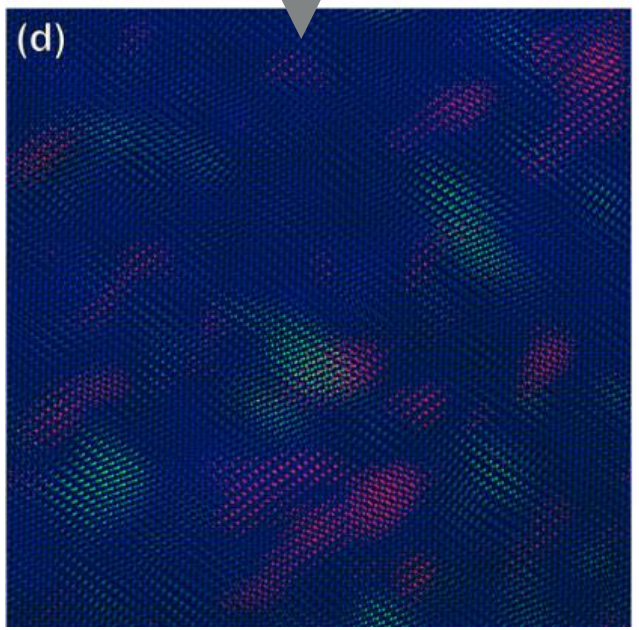

M. Tane, H. Nishiyama, A. Umeda, N. L. Okamoto, K. Inoue, M. Luckabauer, Y. Nagai, T. Sekino, T. Nakano, and T. Ichitsubo
Phys. Rev. Materials **3**, 043604

UNIVERSITY OF TWENTE.

Kinetics of ω phase formation in Ti-21V

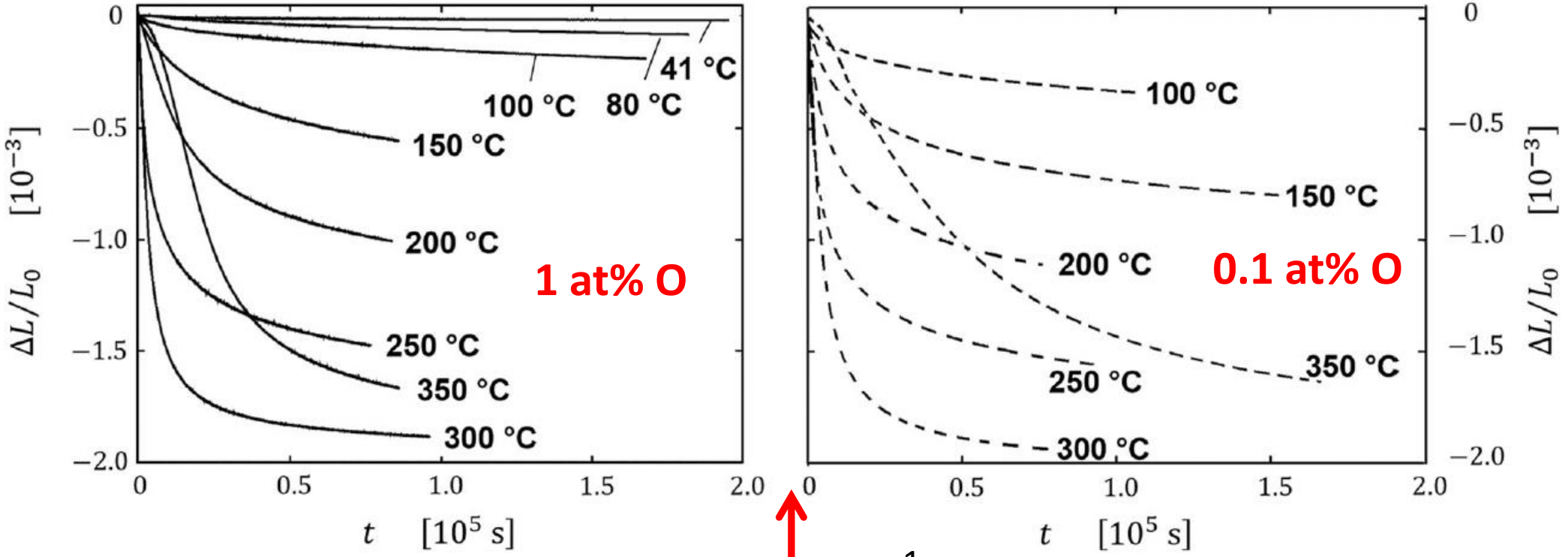

Step 1	Solutionizing: 880 °C for 45 min
Step 2	He-quench to Aging Temperature (30 K/s)
Step 3	Measurement at aging temperature

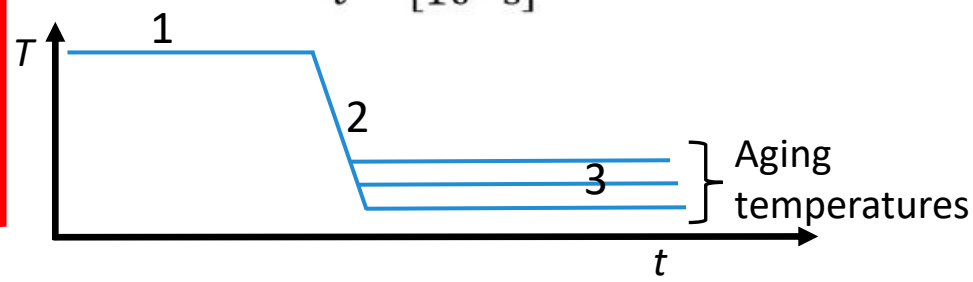

R.J. Enzinger, M. Luckabauer, N.L. Okamoto *et al.* Influence of Oxygen on the Kinetics of Omega and Alpha Phase Formation in Beta Ti–V. Metall Mater Trans A, 2022, https://doi.org/10.1007/s11661-022-06881-1

Kinetics of α phase formation in Ti-21V

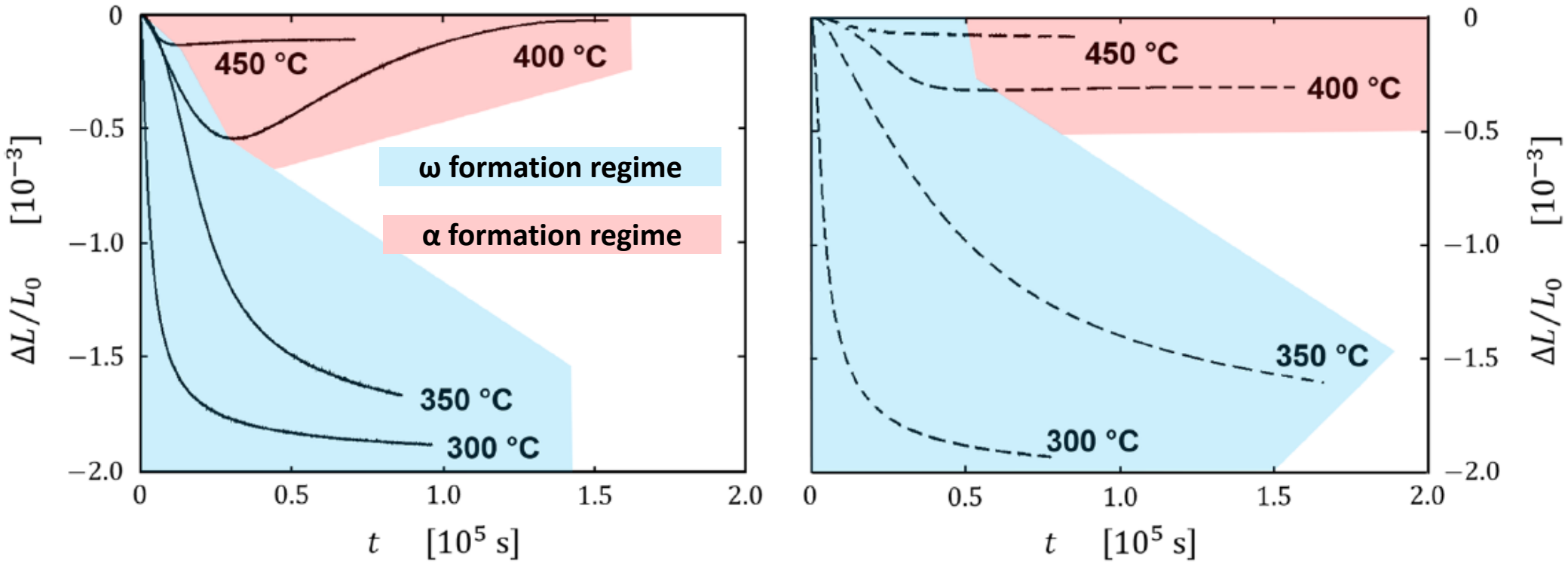

The formation process of both phases is **easily resolved** and can be analyzed in terms of time constants

R.J. Enzinger, M. Luckabauer, N.L. Okamoto *et al.* Influence of Oxygen on the Kinetics of Omega and Alpha Phase Formation in Beta Ti–V. Metall Mater Trans A, 2022, https://doi.org/10.1007/s11661-022-06881-1

TTP diagram of ω phase formation in Ti-21V

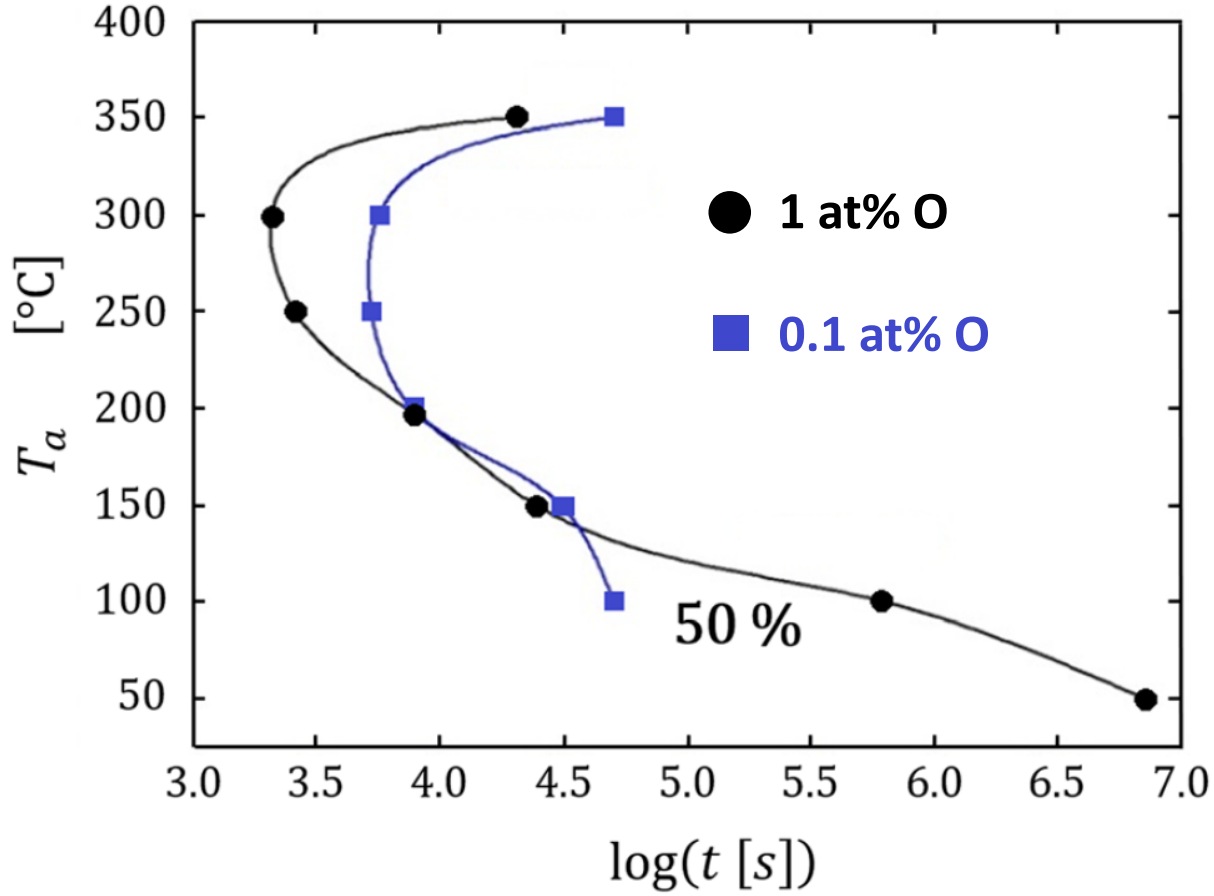

Applying Austin-Rickett kinetics:

The **influence of oxygen** on the formation kinetics of ω was´**quantified for the first time**

Shape also indicates the expected crossover in kinetics of ω formation

R.J. Enzinger, M. Luckabauer, N.L. Okamoto *et al.* Influence of Oxygen on the Kinetics of Omega and Alpha Phase Formation in Beta Ti–V. Metall Mater Trans A, 2022, https://doi.org/10.1007/s11661-022-06881-1

Summary

- Novel dilatometric techniques have the potential **to clarify long standing issues**
- In combination with modern microscopic techniques the method has **unparalleled potential**
- The direct isotherm replication and assessment allows for **time-temperature optimizations** and, consequently **Time and Energy savings**
- **Increase** in **resolution and measurement stability** to allow for isotheral dilatometric measurements **is possible**

Outlook

- Application to **novel** and **established alloy systems** as well application in **fundamental research projects**.

Appendix

Modelling the AW6060 data

2 rate approach (beta' only forms from beta'')

Rate equations for the phases

$$\dot{c}_{\beta''}(t) = k_1\left\{c_0 - \left[c_{\beta''}(t) + c_{\beta'}(t)\right]\right\} - k_2 c_{\beta''}(t)\,, \qquad (1)$$

$$\dot{c}_{\beta'}(t) = k_2 c_{\beta''}(t)\,, \qquad (2)$$

Eq. 1 representing JMAK kinetics with n=1 for the formation β''

Solution with initial zero concentration of both phases:

$$c_{\beta''}(t) = c_0 \frac{k_1}{k_2 - k_1}\left\{\exp(-k_1 t) - \exp(-k_2 t)\right\}, \qquad (3)$$

$$c_{\beta'}(t) = c_0 \frac{1}{k_2 - k_1}\left\{-k_2 \exp(-k_1 t) + k_1 \exp(-k_2 t)\right\} + c_0\,.$$

C_0 is the maximum molar fraction of beta'
(from alloying elements and measurements)

3 rate approach (beta' forms from beta'' and beta' can directly form, presumably at defects)

$$\dot{c}_{\beta'_{\mathrm{dir}}}(t) = k_3\left\{c_0 - \left[c_{\beta''}(t) + c_{\beta'}(t) + c_{\beta'_{\mathrm{dir}}}(t)\right]\right\} \qquad (7)$$

Solutions then read:

$$c_{\beta''}(t) = c_0 \frac{k_1}{k_2 - (k_1 + k_3)}\left\{\exp(-(k_1 + k_3)\,t) - \exp(-k_2\,t)\right\}, \qquad (8)$$

$$c_{\beta'}(t) = c_0 \frac{1}{k_2 - (k_1 + k_3)}$$
$$\left\{-\frac{k_2 k_1}{k_1 + k_3}\exp\left(-(k_1 + k_3)\,t\right)\right. \qquad (9)$$
$$\left. + k_1 \exp(-k_2 t)\right\} + c_0 \frac{k_1}{k_1 + k_3}\,.$$

$$c_{\beta'_{\mathrm{dir}}}(t) = c_0 \frac{k_3}{k_1 + k_3}\left\{1 - \exp(-(k_1 + k_3)\,t)\right\}, \qquad (10)$$

R. Enzinger, E. Hengge, W. Sprengel *et al.* , J Mater Sci **54**, 5083–5091 2019

Modelling the AW6060 data

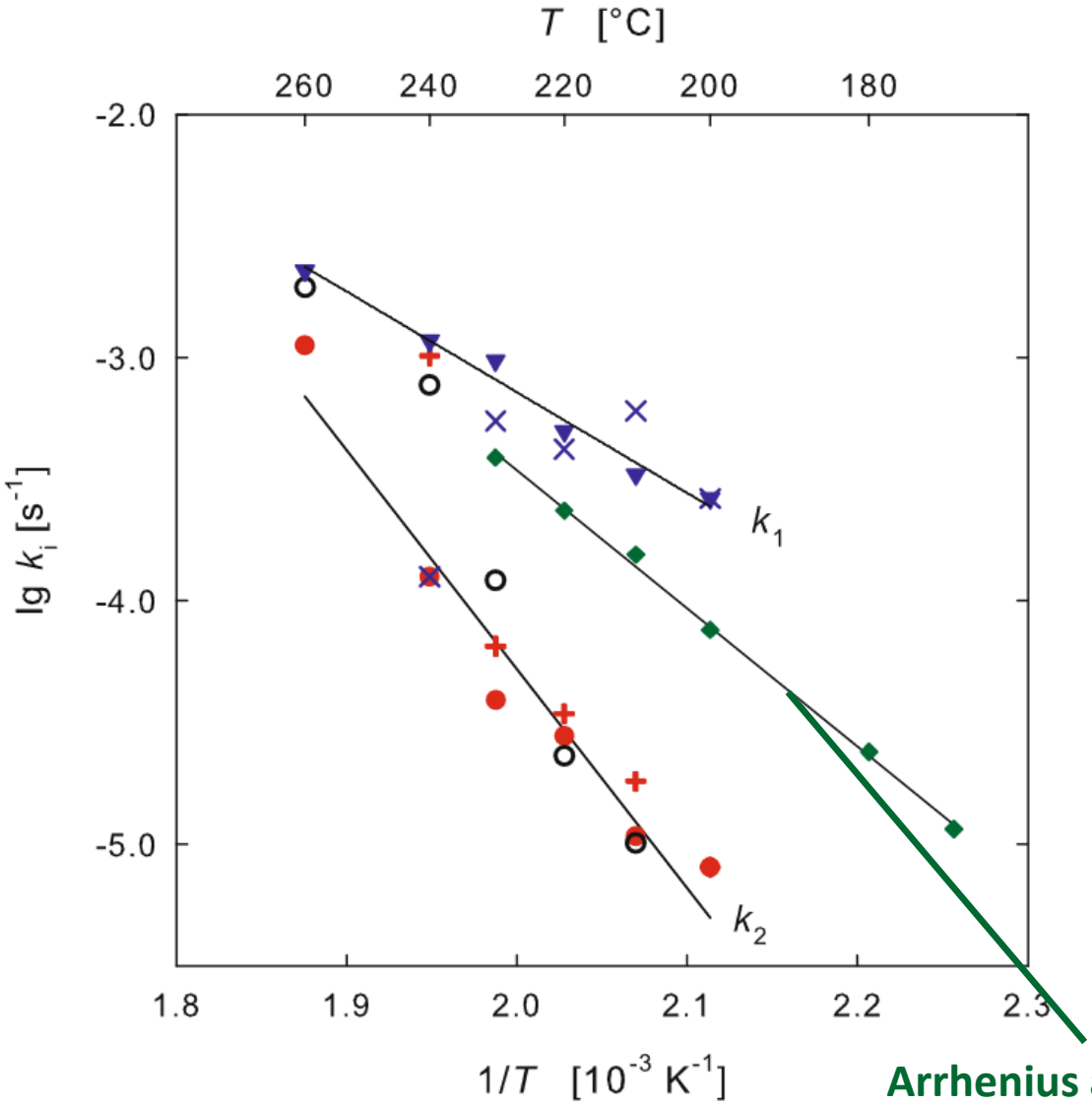

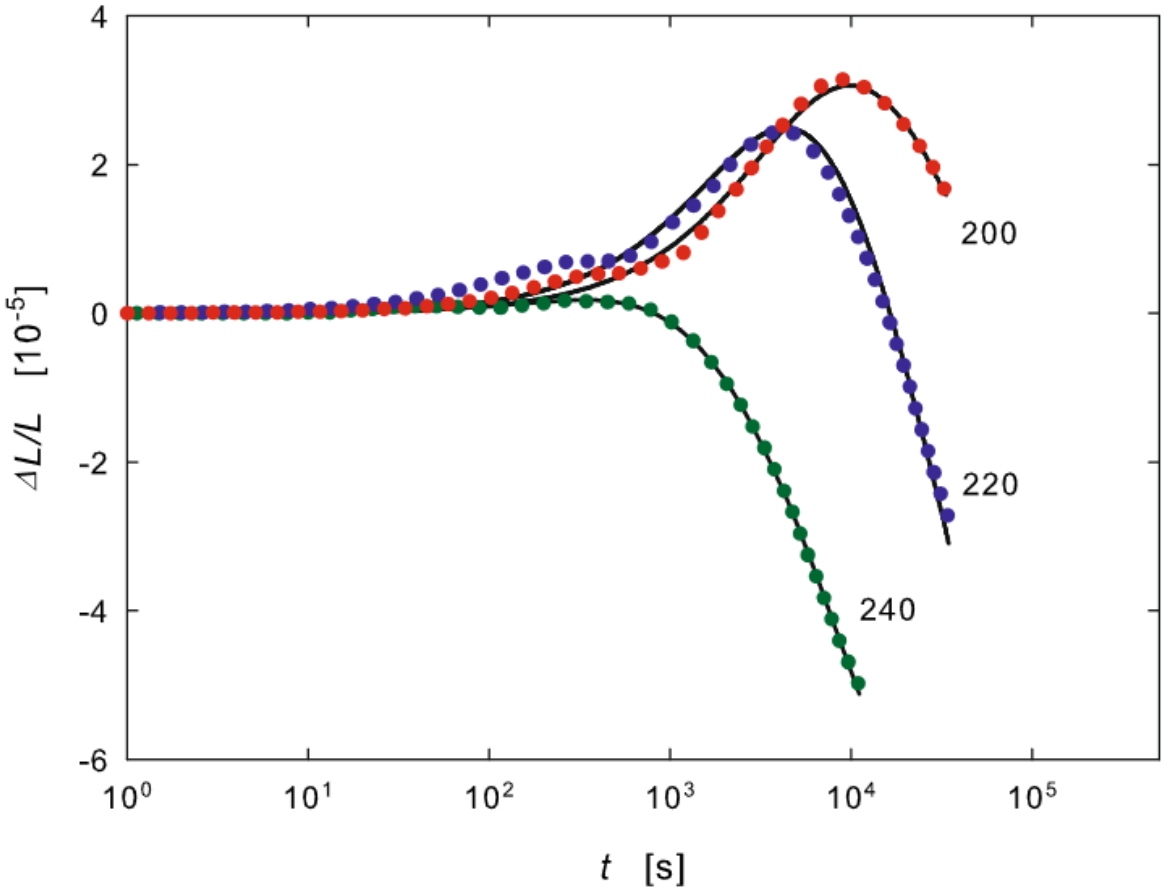

Arrhenius analysis of peak shift

R. Enzinger, E. Hengge, W. Sprengel *et al.* , J Mater Sci **54**, 5083–5091 2019

UNIVERSITY OF TWENTE.

Modelling the TiV data

Length change due to (spinodal) **decomposition**:

$$\left(\frac{\Delta L}{L_0}\right)_{\text{decomp.}} = \frac{1}{3}x_{\beta_l}\left(\frac{a_\beta^3(c_{V,\beta_l},T)}{a_\beta^3(c_{V,0},T)}-1\right) + \frac{1}{3}x_{\beta_r}\left(\frac{a_\beta^3(c_{V,\beta_r},T)}{a_\beta^3(c_{V,0},T)}-1\right) = \left(\frac{\Delta L}{L_0}\right)_{\beta_l} + \left(\frac{\Delta L}{L_0}\right)_{\beta_r}, \quad [1]$$

Length change due to **ω formation**:

$$\left(\frac{\Delta L}{L_0}\right)_{\omega-\text{form.}} = \frac{1}{3}x_\omega\left(\frac{\frac{1}{3}\frac{\sqrt{3}}{2}a_\omega^2(c_{V,\omega},T)c_\omega(c_{V,\omega},T)}{\frac{1}{2}a_\beta(c_{V,0},T)}-1\right) + \frac{1}{3}x_{\beta_r}\left(\frac{a_\beta^3(c_{V,\beta_r},T)}{a_\beta^3(c_{V,0},T)}-1\right) = \left(\frac{\Delta L}{L_0}\right)_{\omega} + \left(\frac{\Delta L}{L_0}\right)_{\beta_r},$$

Length change due to **ω to α transformation**:

$$\left(\frac{\Delta L}{L_0}\right)_{\omega-\text{to}-\alpha-\text{transform.}} = \frac{1}{3}x_\alpha\left(\frac{\frac{1}{2}\frac{\sqrt{3}}{2}a_\alpha^2(T)c_\alpha}{\frac{1}{2}a_\beta^3(c_{V,0},T)}-1\right) + \frac{1}{3}(x_\omega^0-x_\alpha)\left(\frac{\frac{1}{3}\frac{\sqrt{3}}{2}a_\omega^2(c_V^0,\omega,T)c_\omega(c_V^0,\omega,T)}{\frac{1}{2}a_\beta^3(c_{V,0},T)}-1\right) + \frac{1}{3}x_{\beta_r}^0\left(\frac{a_\beta^3(c_{V,\beta_r},T)}{a_\beta^3(c_{V,0},T)}-1\right) = \left(\frac{\Delta L}{L_0}\right)_{\alpha} + \left(\frac{\Delta L}{L_0}\right)_{\omega} + \left(\frac{\Delta L}{L_0}\right)_{\beta_r}. \quad [3]$$

R.J. Enzinger, M. Luckabauer, N.L. Okamoto *et al.* Influence of Oxygen on the Kinetics of Omega and Alpha Phase Formation in Beta Ti–V. Metall Mater Trans A, 2022, https://doi.org/10.1007/s11661-022-06881-1

Modelling the TiV data

Austin-Rickett kinetics:

$$\alpha(t) = 1 - \frac{1}{(k(T)t)^{n_{AR}} + 1}, \qquad [4]$$

Fitting function for the obtained results:

$$f(t) = A\alpha(t) + f_0 = A\left\{1 - \frac{1}{(k(T)t)^{n_{AR}} + 1}\right\} + f_0, \qquad [5]$$

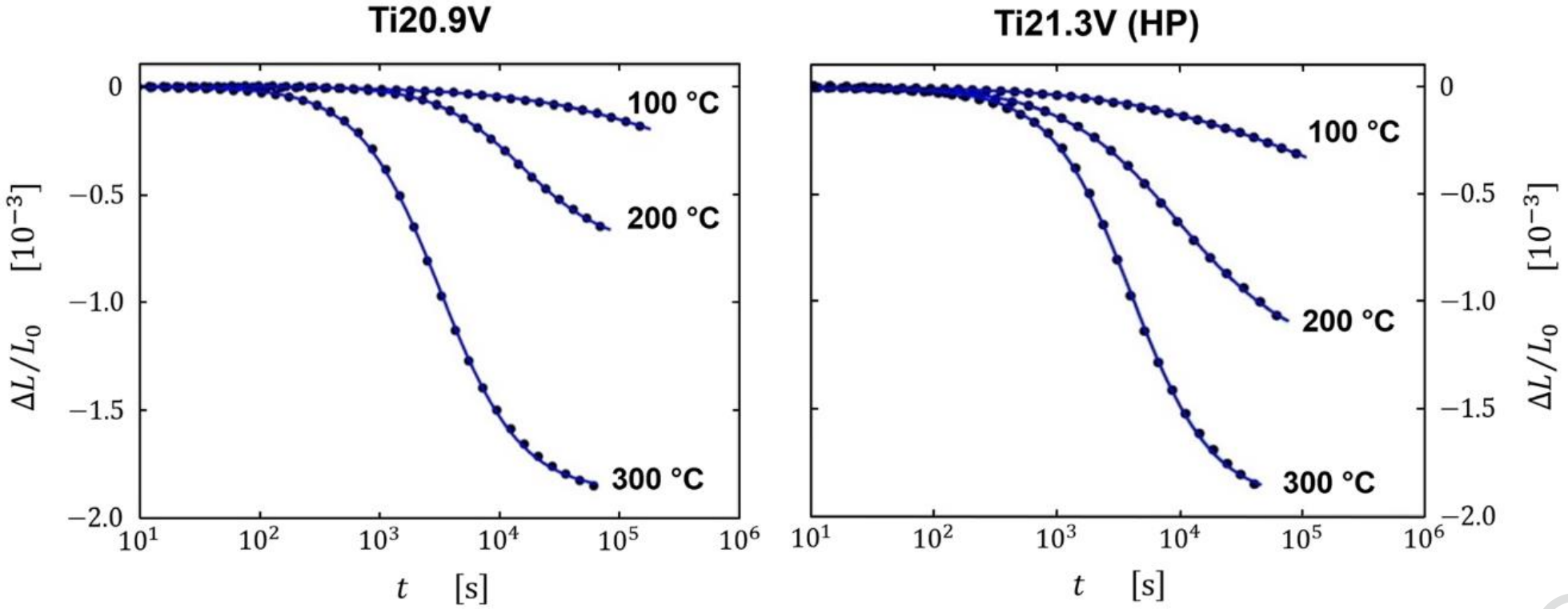

R.J. Enzinger, M. Luckabauer, N.L. Okamoto *et al.* Influence of Oxygen on the Kinetics of Omega and Alpha Phase Formation in Beta Ti–V. Metall Mater Trans A, 2022, https://doi.org/10.1007/s11661-022-06881-1

UNIVERSITY OF TWENTE.

Modelling the TiV data

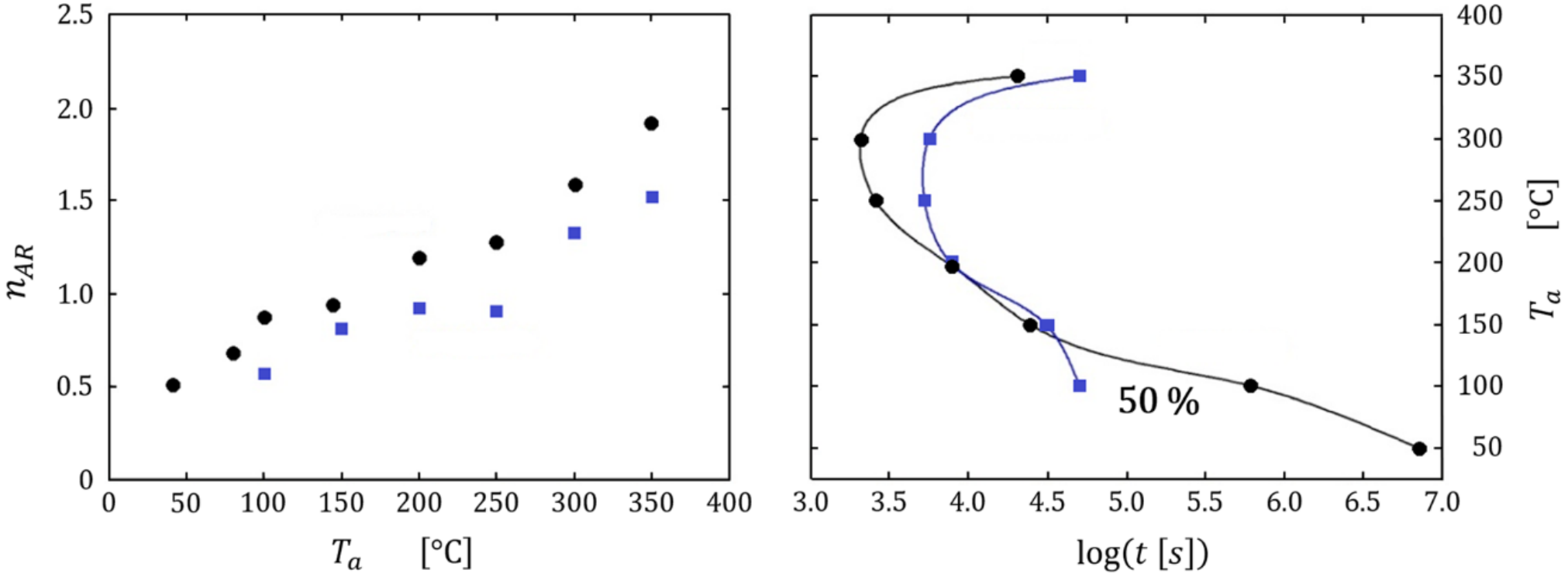

R.J. Enzinger, M. Luckabauer, N.L. Okamoto *et al.* Influence of Oxygen on the Kinetics of Omega and Alpha Phase Formation in Beta Ti–V. Metall Mater Trans A, 2022, https://doi.org/10.1007/s11661-022-06881-1